The stability of embankments reinforced with steel

R. KERRY ROWE

Geotechnical Research Centre, The University of Western Ontario, London, ON N6A 5B9, Canada

AND

BRIAN L.J. MYLLEVILLE

Golder Associates Ltd., 500–4260 Still Creek Drive, Burnaby, BC V5C 6C6, Canada

Received July 9, 1992

Accepted May 19, 1993

The undrained behaviour of embankments constructed on soft cohesive deposits is examined for the case where the embankment is reinforced using steel strips. A finite-element analysis that considers plastic failure of the fill and the foundation, pullout of steel strips, and potential yield of the reinforcement is used to demonstrate how steel reinforcement can improve embankment stability. The effect of strip spacing on the mode of failure and embankment stability is examined for a range of soil strength profiles that involve an increase in undrained shear strength with depth. A simple approach for the analysis of steel-reinforced embankments is proposed and illustrated by means of a worked example. A design based on these simple considerations of bearing capacity and limit equilibrium is then checked against the results of a full finite-element analysis of the problem and found to be slightly conservative.

Key words: reinforcement, steel strips, finite element, limit equilibrium, soft soil, undrained stability.

Le comportement non drainé de remblais construits sur des dépôts mous cohérents est examiné dans le cas où le remblai est armé de bandes d'acier. Une analyse en éléments finis qui prend en compte la rupture plastique du remblai et de la fondation, l'arrachement des bandes d'acier, et la limite élastique potentielle de l'armature est utilisée pour démontrer comment l'armature d'acier peut améliorer la stabilité du remblai. L'effet de l'espacement des bandes sur le mode de rupture et sur la stabilité du remblai est examiné pour une plage de profils de résistance du sol comportant une augmentation de la résistance au cisaillement avec la profondeur. Une approche simple pour l'analyse de remblais armés d'acier est proposée et illustrée au moyen d'un exemple solutionné. Un calcul basé sur ces considérations simples de capacité portante et d'équilibre limite est vérifié par comparaison avec les résultats de l'analyse en éléments finis du problème, et a été trouvé être légèrement trop sécuritaire.

Mots clés : armature, bandes d'acier, éléments finis, équilibre limite, sol mou, stabilité non drainée.

[Traduit par la rédaction]

Can. Geotech. J. **30**, 768–780 (1993)

Introduction

The use of reinforcement as a means of improving the stability of embankments on soft foundations has increased significantly in the past several years. The main thrust has been to use geosynthetic materials as the reinforcement; however, very high modulus materials such as steel meshes, steel bars, and steel strips (Duncan et al. 1987; Fowler et al. 1986; Fukuoka and Goto 1988; Elias and Johnson 1982; and others) have also been successfully used in embankment construction.

This paper examines the undrained behaviour of embankments reinforced with steel strips and constructed on soft clay foundations. Results of finite-element analyses are used to examine the influences of steel strip spacing on embankment behaviour. A design methodology is then presented. This methodology is directed at providing a quick means of estimating the potential benefits of using steel strip reinforcement.

The authors are not aware of any well-documented case history involving the use of steel strip reinforcement for embankments on soft clay against which the analysis and proposed design methods can be tested. It is, however, noted that the techniques adopted in the paper have been successfully used in predicting the behaviour of instrumented geotextile-reinforced embankments on soft foundations (e.g., Rowe and Soderman 1984; Rowe et al. 1984; Mylleville and Rowe 1993). It is hoped that the present paper will generate interest concerning the potential use of steel strips as reinforcement for embankments and that the resulting field experience can be used to test and refine the design methodology, described herein.

Problem description

The short-term (friction angle $\phi = 0°$) stability of steel strip reinforced embankments constructed on soft cohesive deposits is examined. As illustrated in Fig. 1, the granular embankments have a crest width B, and fill thickness H, and are constructed on soft clay deposits of depth D, which are underlain by a rigid base. The embankment is reinforced with a single layer of steel strips similar to those used in reinforced earth (R) walls (Vidal 1969) of width w, thickness t, and centre to centre spacing S (see also section A–A, Fig. 1). The reinforcing strips are located above the clay–fill interface (i.e., within the fill) to allow mobilization of frictional resistance on both the top and bottom surfaces of the strips. Unless otherwise noted, the finite-element results were obtained assuming a single layer of steel reinforcing strips located 375 mm above the clay–fill interface for an embankment with 2:1 side slopes ($n = 2$ in Fig. 1).

The embankments are constructed on soft clay deposits where the undrained shear strength increases linearly with depth (i.e., where ρ_c is the nominal rate of increase in undrained strength with depth) from some nominal surface value c_{uo}, as shown in Fig. 1.

Printed in Canada / Imprimé au Canada

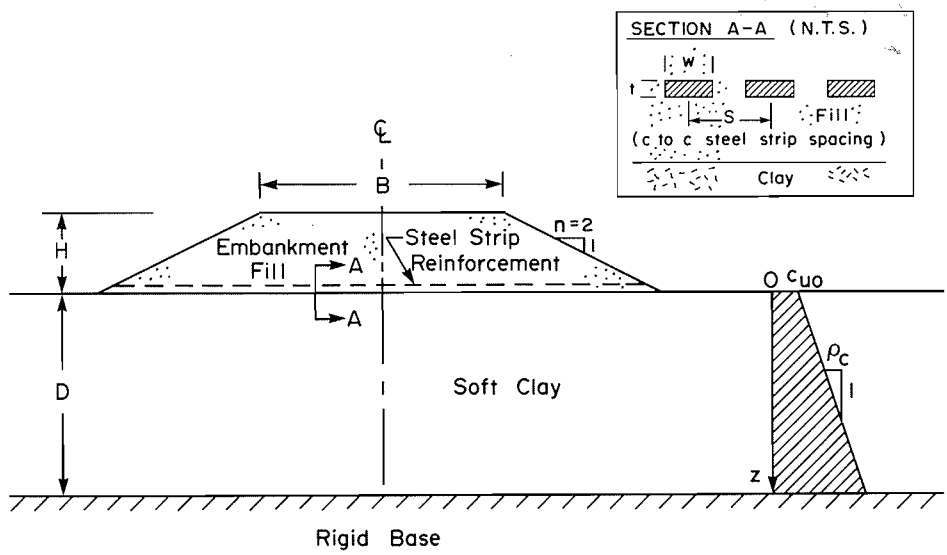

FIG. 1. Reinforced embankment on soft clay deposit. c to c, centre to centre. NTS, not to scale.

Partial factors and limit state design

There are two basic approaches to the design of embankments on soft clay foundations.

The conventional approach commonly adopted for unreinforced embankments under undrained conditions is to determine the factor of safety for a given design height using nominal soil parameters (usually the expected values of the strength or unit weight of the soil) and calculating the ratio of the restoring moment to the overturning moment. This "factor of safety" is expected to exceed some minimum factor of safety (often 1.3–1.5 for embankments in noncritical situations). However, when one deals with a reinforced embankment where failure may involve not only failure of the soil but also failure of the soil–reinforcement interface and (or) yield of the reinforcement itself, this approach may not provide a meaningful indication of the amount of reinforcement required to achieve a given design height.

An alternative approach, which can give the same results for an unreinforced embankment but also allows a rational evaluation of the amount of reinforcement that is needed to achieve a given design height, is to adopt a limit states design approach. With this approach, partial factors are applied to the nominal strength of the soil, the soil–reinforcement interface strength, and the strength of the reinforcement to give factored strength parameters. In addition, load factors are applied to the load tending to cause failure. Thus, the factored strength parameters are obtained by multiplying the nominal strength parameters (e.g., undrained strength c_u, and tangent of friction angle ϕ) by partial factors that are typically less than unity. The factored loads are obtained by multiplying the nominal loads (e.g., unit weight of the fill) by a load factor that is greater than (or equal to) one. Depending on the situation and the perceived uncertainty, different partial factors and load factors may be applied to the different components. With this approach one usually seeks a level of reinforcement at which the restoring moment (calculated using factored strength parameters) is in equilibrium with the overturning moment.

For an unreinforced-embankment analysis, the approach described in the previous paragraph would give the same allowable embankment height (for a given desired factor of safety) as the conventional approach if the partial factor applied to the soil strength is taken to be the reciprocal of the desired factors of safety and the nominal unit weight is used. The typical justification for this approach is that the engineer has control of the unit weight of the fill but not of the shear strength of the foundation, and so the greatest uncertainty may be associated with the soil shear strength. However, if one wished to follow a full limit-states design philosophy, then the limit equilibrium analysis should be performed using loads (e.g., fill weights) that have been factored up (by multiplying nominal values by a load factor which is greater than unity) as well as strength parameters that have been factored down (by multiplying nominal values by partial factors less than unity).

To illustrate the use of limit-states design as applied to the design of steel-reinforced embankments the examples presented in this paper make use of load and partial factors taken from the Ontario Highway Bridge Design Code (Ministry of Transportation of Ontario 1983). Partial factors of 0.65 and 0.8 are applied to the undrained strength of the clay foundation and tangent of the angle of internal friction of fill, respectively. A load factor of 1.25 is applied to the unit weight of the fill where it is used to assess overturning moment; however, a load factor of 1.0 is used for assessing the pullout resistance at the reinforcement–fill interface. The strength of the steel strip reinforcement is also factored using appropriate code clauses. Using this approach and these partial factors, the conventional factor of safety of an unreinforced embankment is about 1.9. The finite-element analyses described in this paper were performed using parameters factored as described above.

Finite-element model

To understand the effects of using a particular form of reinforcement, it is necessary to properly model the response of the entire reinforced embankment system as it is constructed to failure. A small-strain finite-element program AFENA (Carter 1985) was modified by the authors to allow consideration of pullout for steel strips. Plastic failure within the soil was modelled using an elastoplastic formulation (e.g., Ziekiewicz 1977). The specific model adopted by the

TABLE 1. Range of nominal foundation (soft clay) properties considered

Surface undrained shear strength c_{uo} (kPa)	5–30
Rate of increase in strength with depth ρ_c (kPa/m)	1–2.5
Unit weight γ (kN/m^3)	16.5
Coefficient of earth pressure at rest K_o'	0.6
Strength to effective vertical stress ratio c_u/σ'_{vo}	0.15–0.40
Undrained Young's modulus shear strength ratio E_u/c_u	125
Undrained Poisson's ratio ν_u	0.48
Depth of soft deposit D (m)	15

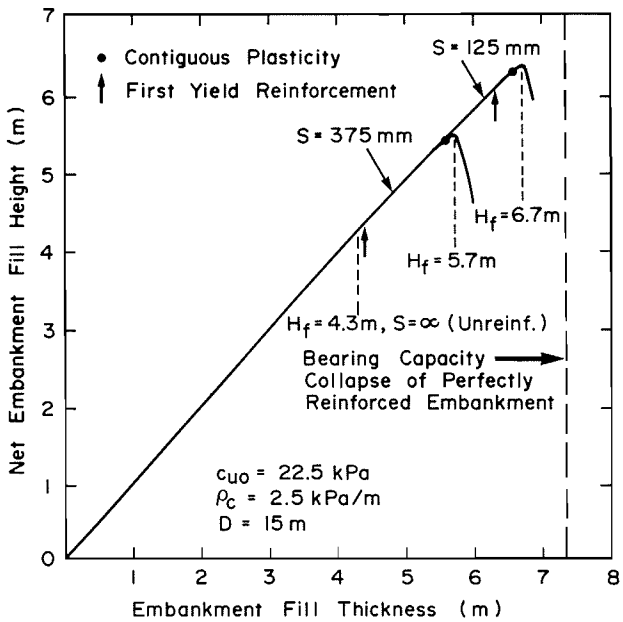

FIG. 2. Net embankment fill height vs. embankment fill thickness (plotted for a point located directly beneath the shoulder of the embankment at the clay-fill interface). H_f, fill thickness at failure of embankment.

authors assumes a Mohr–Coulomb failure criterion together with a flow rule of the form proposed by Davis (1968).

The reinforcement in the embankment was modelled using bar elements where the axial stiffness is a representative value per unit width of the embankment. When modelling the behaviour of reinforced soil using strip reinforcement, it is necessary to consider several failure mechanisms (see Rowe and Mylleville 1988) at the soil–reinforcement interface, one of which includes pullout of the reinforcement. Since pullout of the strip reinforcement represents a three-dimensional situation, it can only be approximately modelled in a two-dimensional analysis (e.g., Naylor and Richards 1978; Rowe and Mylleville 1988). The approach implemented by the authors involves an interface element that has a node above the reinforcement, a node on the reinforcement, and a node below the reinforcement. Since the reinforcing strips do not cover the entire area of soil, the Mohr–Coulomb parameters were adjusted to take into account the actual surface area, per unit width of the embankment, which is in contact with the soil. Specific details regarding the finite-element formulation adopted by the authors are given by Rowe and Mylleville (1988).

A finite-element mesh with 4247 degrees of freedom was used to perform the small-strain analyses. The case of a rough rigid footing was used to check that the refinement of the mesh was adequate. Collapse loads for highly reinforced embankments agreed to better than 7% with those obtained for rigid footings from plasticity theory. Construction of the reinforced embankments was simulated by incrementally applying the weight of rows of elements. In total, up to 14 lifts (rows of elements) and a total of up to 250 load steps were adopted to simulate embankment construction.

Parameter selection

Table 1 provides a brief review of the nominal parameters used for the various components of the reinforced embankments discussed herein. Factored parameters were used in the analysis as previously discussed.

Embankment fill

The nominal value of unit weight adopted for the embankment fill was 20 kN/m^3. The angle of internal friction used was $\phi = 36°$ (nominal). The value of Poisson's ratio was taken to be $\nu = 0.35$.

The nonlinear stiffness characteristic of the embankment fill was modelled using Janbu's equation in the finite-element analyses discussed herein, viz.

$$\frac{E}{P_a} = K\left(\frac{\sigma_3}{P_a}\right)^m$$

where E is Young's modulus (stiffness), P_a is atmospheric pressure, σ_3 is minor principal stress, K is a material parameter (=100), and m is material parameter (=0.5).

Plastic failure was modelled using a Mohr–Coulomb failure criteria and a nonassociated flow rule with dilatancy angle of zero.

Reinforcement

The reinforcing steel strips considered here are ribbed, 50 mm wide, and 5 mm thick. The steel used had a Young's modulus of 200 GPa, with a yield strength, σ_y, of 350 MPa and an ultimate tensile strength, σ_{UTS}, of 490 MPa. A centre to centre spacing S between steel strips of 125 and 375 mm was examined.

Effect of steel strip spacing on embankment behaviour

The amount of reinforcement (i.e., steel strip spacing) may have a substantial effect on the behaviour of a reinforced embankment. For example, Fig. 2 shows the variation in net embankment fill height versus embankment fill thickness at a point located directly beneath the shoulder of the embankment at the clay–fill interface for centre to centre steel strip spacings of 375 and 125 mm. Both cases involve a cohesive deposit with a nominal surface undrained shear strength c_{uo} of 22.5 kPa and a nominal rate of increase in strength with depth, ρ_c, of 2.5 kPa/m (with the foundation and

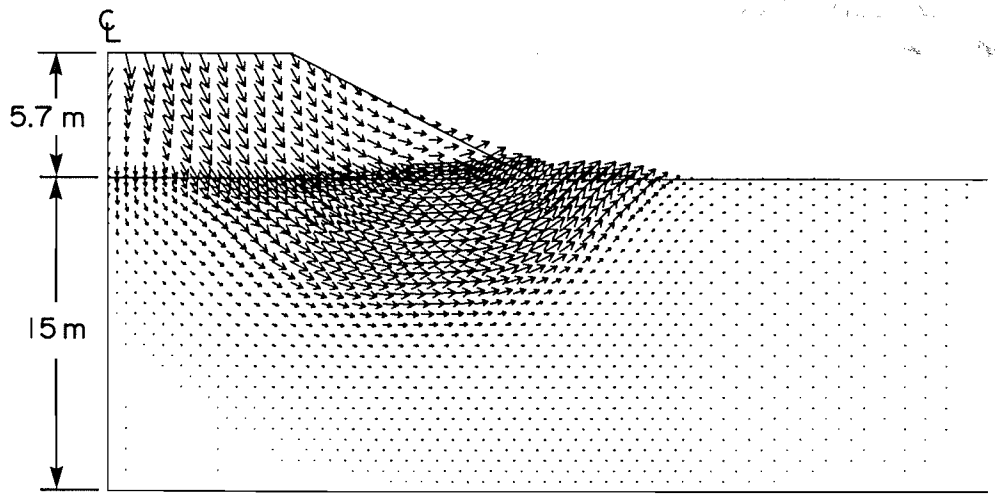

FIG. 3. Velocity field at failure; S = 375 mm.

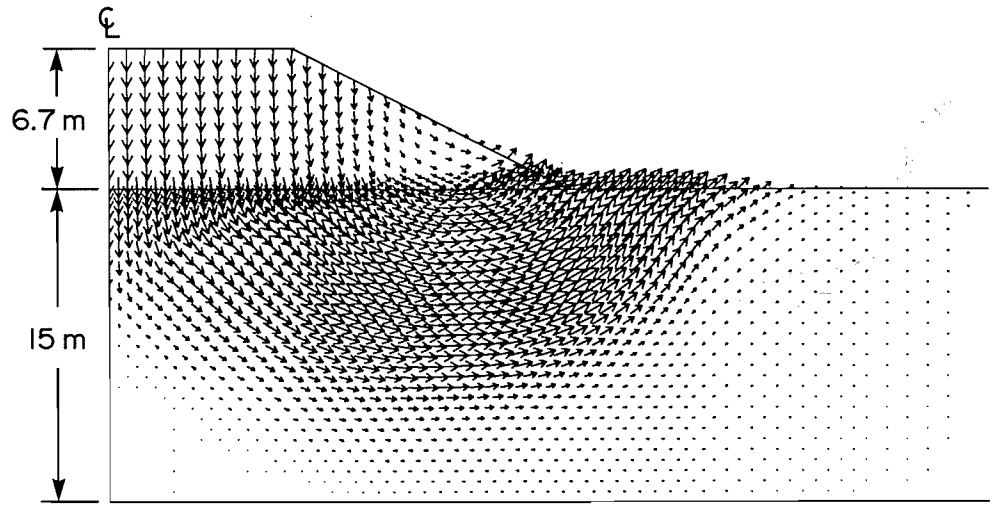

FIG. 4. Velocity field at failure; S = 125 mm.

fill strength and fill unit weight being factored for a limit state design as previously discussed).

Referring to Fig. 2, the maximum value of net embankment fill height (or top of each curve) corresponds to failure of the entire embankment system. Failure of the reinforced embankment is defined as the height at which the increment in vertical displacement is equal to or exceeds the increment in fill thickness just added. The addition of more fill will not result in a net increase in embankment fill height. For heavily reinforced embankments, the fill thickness at failure is very close to the plasticity collapse fill thickness at which uncontained plastic flow occurs. This is in contrast to typical geotextile-reinforced embankments where the failure height may be considerably less than the collapse height based on plasticity theory (see Rowe and Soderman 1987*a*).

For a steel strip spacing S of 375 mm, the embankment fill thickness at failure is equal to 5.7 m. This represents a 33% improvement in allowable fill thickness compared to the unreinforced ($S = \infty$) fill thickness of 4.3 m. A threefold increase in the amount of steel (i.e., a spacing S of 125 mm) results in an embankment fill thickness at failure equal to 6.7 m, representing a 56% increase in allowable fill thickness when compared to the unreinforced case. As one would expect, increasing the amount of reinforcement by a factor of three has improved the embankment performance and increased the allowable fill thickness. However, it should be noted that the allowable fill thickness obtained using a steel strip spacing S of 125 mm is approaching the maximum fill thickness that can be achieved for a perfectly reinforced embankment (i.e., fill thickness corresponding to bearing capacity collapse of a perfectly reinforced embankment determined as described by Rowe and Soderman 1987*b*) as shown in Fig. 2. Also shown in Fig. 2 is the fill thickness that corresponds to the point at which the reinforcement first yields. In both analyses, some yield of the reinforcing strips does occur (based on factored properties for the steel, fill and foundation); however, for the closer spacing (i.e., S = 125 mm) yield occurs just prior to failure.

Figure 3 shows the velocity field corresponding to the onset of failure of the embankment reinforced with steel strips at a spacing of 375 mm. The arrows indicate the direction and relative magnitude of soil movement at failure. In this case, the failure mechanism involves a combination of reinforcement yield, some pullout of the reinforcement, and general foundation soil failure. To allow an appreciation of the effect of increasing the amount of reinforcement (i.e., adopting a closer strip spacing) on the failure mechanism, Fig. 4 shows the velocity field at failure for an embankment reinforced with steel strips at a spacing of 125 mm. A comparison of the results for S = 125 mm (Fig. 4) with

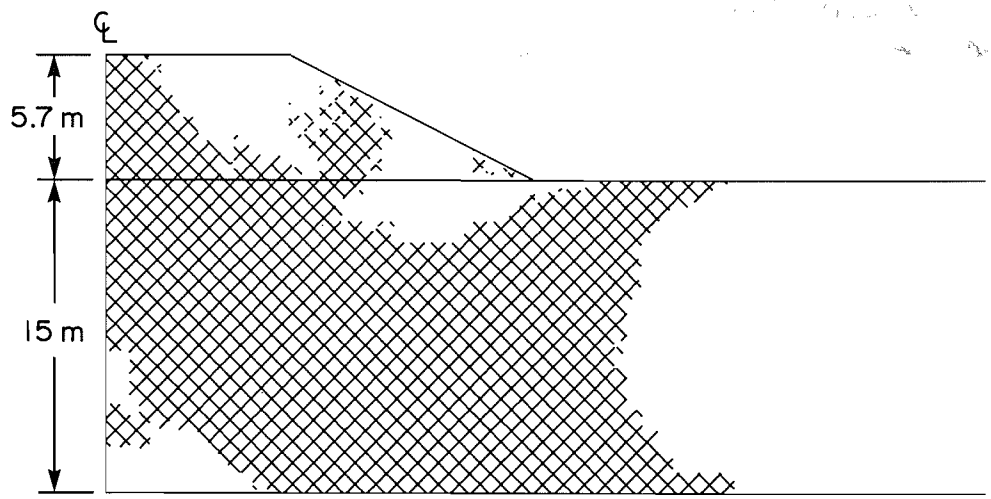

FIG. 5. Plastic region at failure; S = 375 mm.

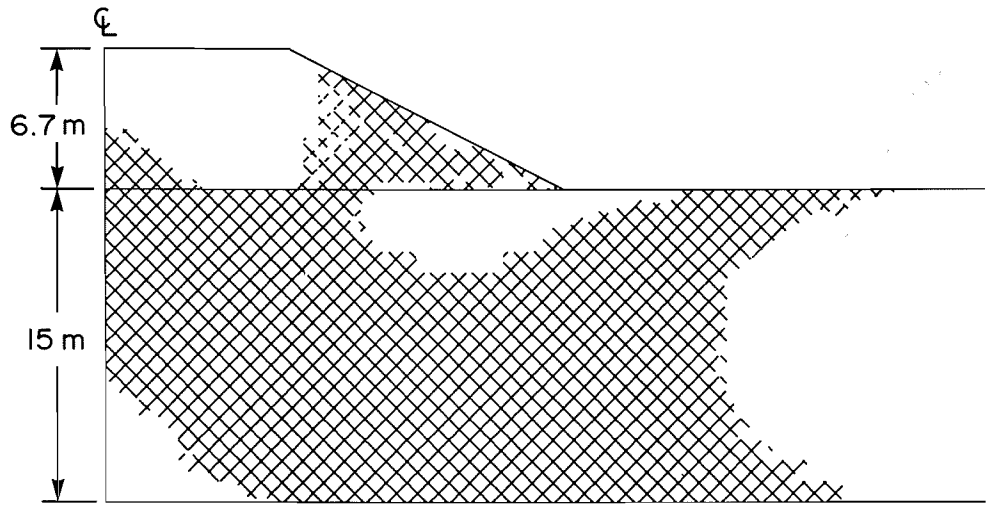

FIG. 6. Plastic region at failure; S = 125 mm.

those for S = 375 mm (Fig. 3) shows several differences. Firstly, the increased amount of reinforcement has resulted in an increase in failure height by about 1 m. Secondly, the failure mechanism is forced much deeper into the foundation soil for the case of the closer strip spacing. Thirdly, the increased amount of reinforcement for S = 125 mm has virtually eliminated the horizontal component of displacement within the embankment fill. The embankment fill is essentially moving vertically downward as a rigid block (see Rowe and Mylleville 1988, and Mylleville and Rowe 1988 for a more detailed discussion).

The fact that the more heavily reinforced embankment tends to behave as a rigid block can also be seen if one examines the plastic regions at failure shown in Figs. 5 and 6 for steel strip spacings of 375 and 125 mm, respectively. The cross-hatched areas represent that zone of soil that has reached its shear strength at the onset of failure. Examining the embankment fill between the centreline and shoulder for the 125 mm strip spacing (Fig. 6) it can be seen that there is considerably less plasticity, which is consistent with the fact that the heavily reinforced embankment fill is essentially moving downward as a rigid block. The small amount of plasticity beneath the centreline is due to the fact that some yielding of the reinforcement has occurred just prior to failure (see also Fig. 2).

The point about which rotation is occurring between the shoulder and the toe of the embankment in Figs. 3 and 4 corresponds to that point where the applied pressure is equal to the surface bearing capacity of 5.14 c_{uo}. The behaviour of the heavily reinforced embankment just discussed provides some justification for adopting an approximate method proposed by Rowe and Soderman (1987*b*) for evaluating the maximum embankment height that can be achieved with reinforcement. The application of this method for steel-reinforced embankments is outlined in a later section of this paper.

Figure 7 shows the relationship between allowable pressure (i.e., γH, where γ is the nominal fill unit weight 20 kN/m^3, and H is the fill thickness obtained from finite-element analyses using factored parameters) and nominal surface undrained shear strength c_{uo}. The undrained shear strength at the surface ranges from 5 to 30 kPa; and the rate of increase in strength with depth, ρ_c, is 2.5 kPa/m. The corresponding relationship for ρ_c = 1 kPa/m is shown in Fig. 8.

The curves shown in Figs. 7 and 8 were obtained from finite-element analyses performed using factored parameters

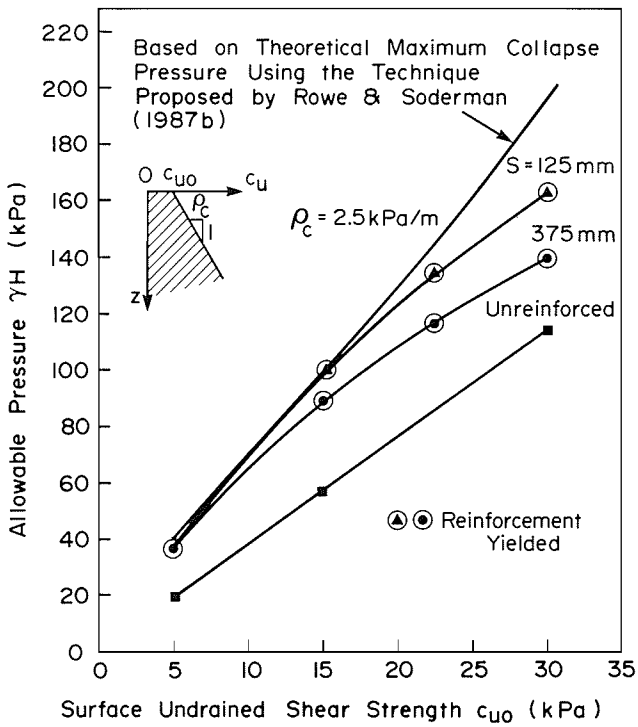

FIG. 7. Allowable embankment height H as a function of foundation strength and reinforcement (ρ_c = 2.5 kPa).

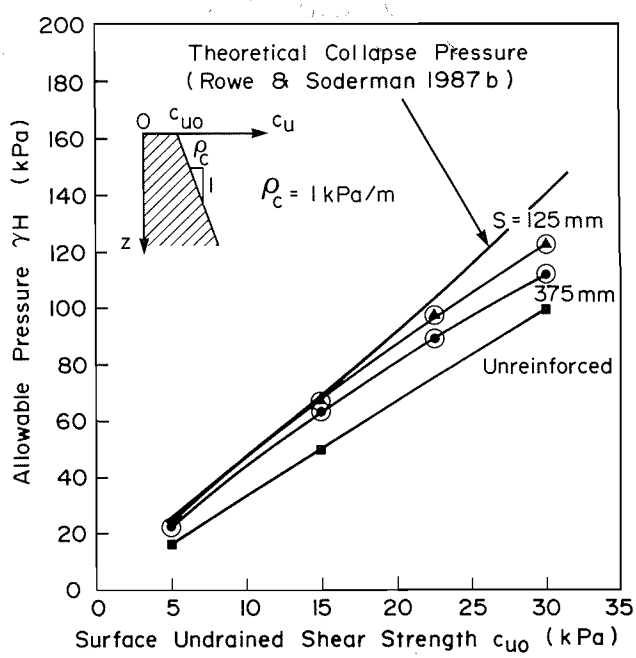

FIG. 8. Allowable embankment height H as a function of foundation strength and reinforcement (ρ_c = 1 kPa).

(Ministry of Transportation of Ontario 1983). Three reinforcement spacings were considered: unreinforced ($S = \infty$), S = 375 mm, and S = 125 mm. Also shown is the curve of theoretical collapse pressure based on plasticity theory, which provides an upper bound to the maximum improvement that can be realized using any form of reinforcement (based on Rowe and Soderman 1987*b*).

Referring to Figs. 7 and 8, it will be noted that for the lower foundation strengths, the allowable pressures obtained for the two steel strip spacings considered are very close to or at the theoretical collapse pressure predicted based on plasticity theory using the hand-calculation method proposed by Rowe and Soderman (1987*b*). Provision of additional reinforcement does not result in an increase in allowable fill thickness. For the cases where there is no reinforcement yield, the reinforced embankment behaves very similarly to a rigid footing at failure. There is significant slip beneath the fill–clay interface as the underlying foundation soil is squeezed out from beneath the heavily reinforced embankment.

As the foundation strength is increased, the allowable fill thickness at failure is controlled by the strength of the reinforcement per metre width.

Comparing the results shown in Figs. 7 and 8 for a given steel spacing, it can be seen that compared to the unreinforced case, the steel strip reinforcement results in a greater improvement in allowable fill thickness for the higher rate of increase in strength with depth (i.e., ρ_c = 2.5 kPa/m). In other words, the amount of improvement realized by using reinforcement is highly influenced by the rate of increase in strength with depth. This is consistent with previous findings by Rowe and Soderman (1985) related to geosynthetic reinforcement (i.e., relatively extensible reinforcement).

An approach for the evaluation of embankment stability

Assuming that a design embankment height has been established based on the proposed function of the embankment, the analysis of undrained stability for an (potentially reinforced) embankment involves three basic steps.

(1) *Stability of embankment without reinforcement*

Assess whether an unreinforced embankment could be constructed to the desired height H. This can be assessed based on a conventional limit equilibrium analysis. If the shear strength parameters and unit weight have been factored in accordance with limit-state design, then the ratio of restoring moment to overturning moment must be greater than or equal to one for the unreinforced embankment to be judged satisfactory. In this case there is no need for reinforcement and the analysis stops. If this ratio is less than one, then the embankment cannot be safely constructed to the desired design height without reinforcement, or some other form of soil improvement or staged construction.

(2) *Bearing capacity limits for a heavily reinforced embankment*

Assess whether it is possible to achieve the desired design height by use of soil reinforcement. This assessment is based on bearing capacity considerations and will be described later in the text. If the design height exceeds the maximum that can be achieved using reinforcement, then some other form of soil improvement and (or) stage construction would be required (possibly in conjunction with soil reinforcement).

(3) *Stability of a reinforced embankment*

If the desired design height can be achieved using soil reinforcement (as established in step 2), then evaluate the amount of reinforcement required to achieve the desired grade by means of limit equilibrium calculations that consider the limit equilibrium of both the soil and the soil–reinforcement system.

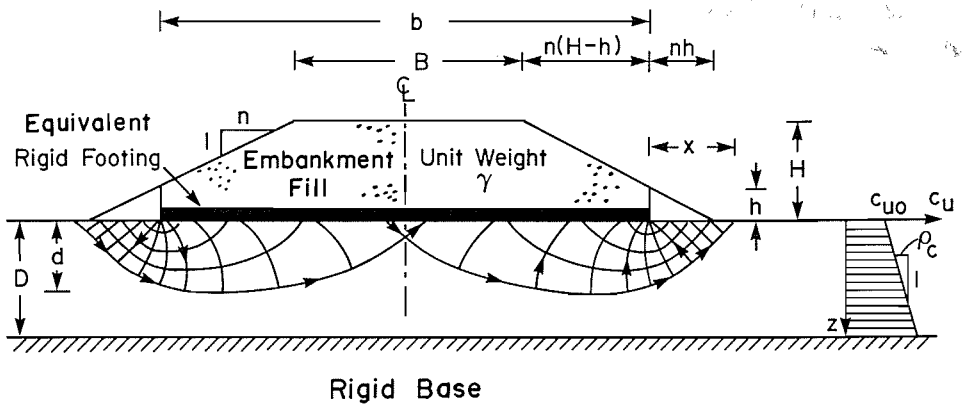

FIG. 9. Definition of variables used to estimate the collapse height for a perfectly reinforced embankment (modified from Rowe and Soderman 1987*b*).

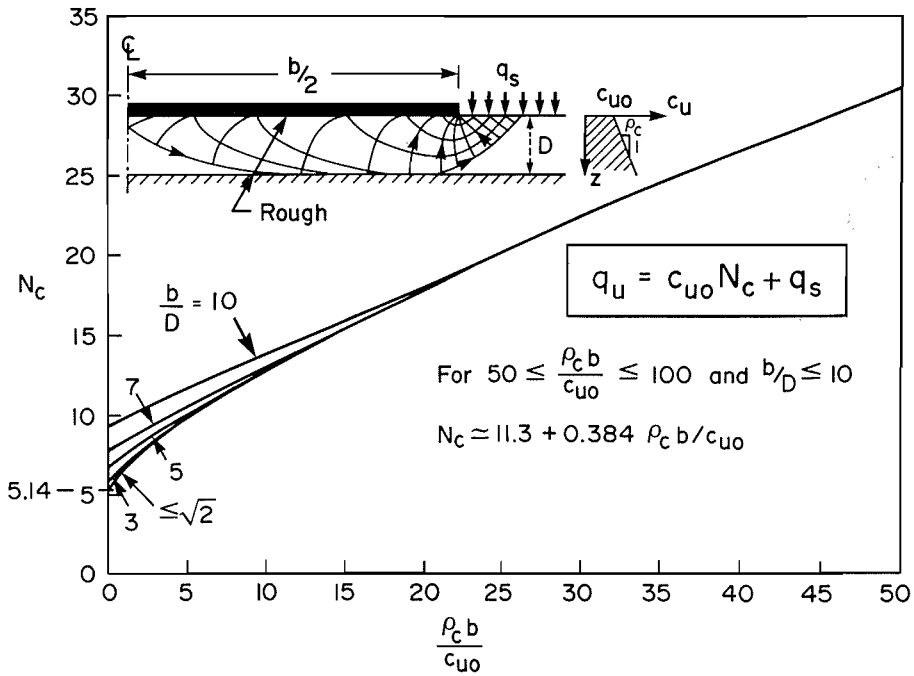

FIG. 10. Bearing capacity factor for nonhomogeneous soil (modified from Rowe and Soderman 1987*b*).

The foregoing three steps apply for all forms of reinforcement. However, there is a major difference between steel strip reinforcement and geosynthetic (i.e., geotextile and geogrid) reinforcement associated with step 3. In the case of planar geotextile reinforcement, pullout (or anchorage) of the reinforcement is generally not a controlling factor, since the maximum force that can be developed is often controlled by serviceability considerations and the maximum allowable strain in the reinforcement (e.g., see Rowe and Soderman 1985, 1987*a*). Steel reinforcement strips have a high stiffness (relative to geosynthetics), and the maximum force that can be developed is typically controlled either by pullout (anchorage) of the steel strip or yield of the steel. It is noted that steel yields at very low strain but, because of its ductility, tensile failure does not occur until strains are reached which are higher than those attainable for many forms of high-strength geosynthetic reinforcement.

Steps 1 and 3 both involve limit equilibrium calculations and will be discussed together following the discussion of the evaluation of the bearing capacity of a heavily reinforced embankment.

As with all geotechnical analyses, the techniques described herein should only be used by an experienced geotechnical engineer capable of both assessing the applicability of the analysis for a given situation and selecting appropriate soil parameters.

Bearing capacity analysis

A simple technique for estimating the maximum improvement in collapse load for a reinforced embankment has been developed by Rowe and Soderman (1987*b*). The method, which will be briefly outlined here, considers the effect of increasing undrained shear strength with depth as well as the effect of the relative thickness of the underlying soil deposit. Since a reinforced embankment can never be reinforced beyond the point of being rigid, these solutions place a limit on the improvement in stability that can be achieved using high-strength modulus reinforcement.

Since an embankment will generally be trapezoidal in shape and the plasticity solutions are for a rigid footing of width b, an approximation must be made to determine the equivalent width of the embankment (see Fig. 9 for defini-

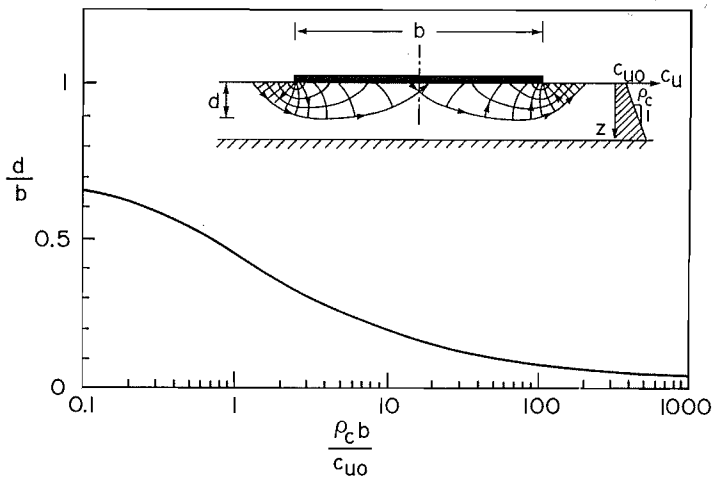

FIG. 11. Effect of nonhomogeneity on depth of the failure zone beneath a rough rigid footing (modified from Rowe and Soderman 1987*b* and based on results obtained by Matar and Salençon 1977).

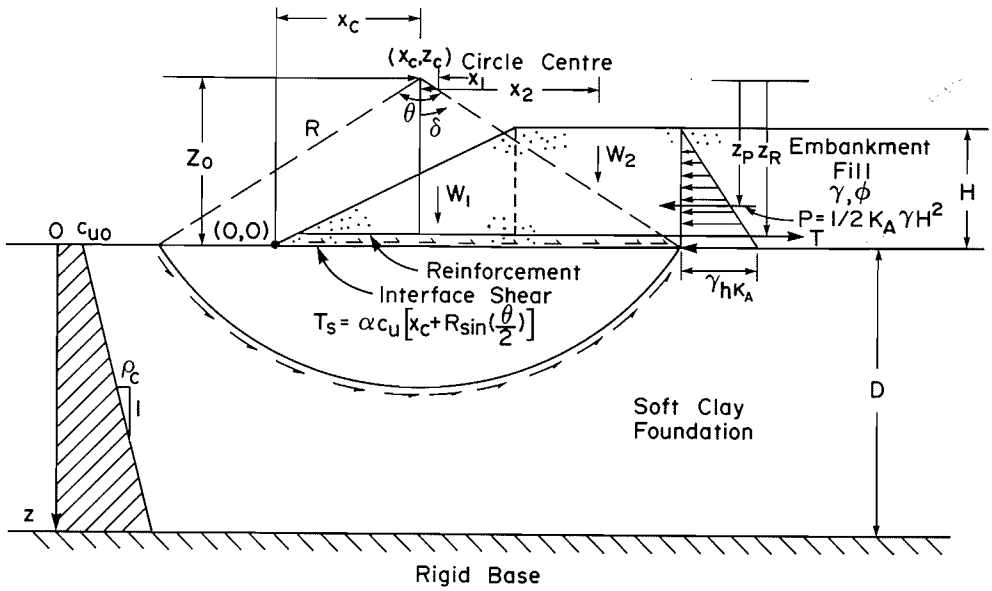

FIG. 12. Schematic of reinforced embankment to be analyzed using limit equilibrium.

tion of variables). From plasticity considerations, the pressure at the edge of a rigid footing is $(2 + \pi)c_{uo}$, where c_{uo} is the undrained strength directly beneath the footing. It is assumed here that the effective width b of the footing will extend between the points on either side of the embankment when the applied pressure γh is equal to $(2 + \pi)c_{uo}$. Thus

$$[1] \quad h = \frac{(2+\pi)c_{uo}}{\gamma}$$

and hence (from Fig. 9)

$$[2] \quad b = B + 2n(H - h)$$

where B is the crest width, H is the embankment height, and n is the cotangent of the slope angle.

The bearing capacity q_u of the rigid footing of width b is given by

$$[3] \quad q_u = N_c\, c_{uo} + q_s$$

where q_s is a uniform surcharge pressure applied to the soil surface outside of the footing width. The bearing capacity factor N_c is determined using Fig. 10. Inspection of Fig. 9 shows that the triangular edge of the embankment provides a surcharge that would increase stability, and hence an estimate of q_s in terms of the pressure applied by this triangular distribution is required.

Figure 11 shows the depth d to which the failure mechanism is expected to extend. The lateral extent of the plastic region involved in the collapse of a rigid footing extends a distance x from the footing, where x is approximately equal to the minimum of d as determined from Fig. 11 and the actual thickness of the deposit D, i.e.,

$$[4] \quad x = \min(d,D)$$

Thus distributing the applied pressure due to the triangular distribution over a distance x gives

$$[5a] \quad q_s = \frac{n\gamma h^2}{2x} \quad \text{for} \quad x > nh$$

and

$$[5b] \quad q_s = \frac{(2nh - x)\gamma h}{2nh} \quad \text{for} \quad x \le nh$$

The value of q_u may then be compared with the average applied pressure q_a due to the embankment over the width b, viz.

$$[6] \quad q_a = \frac{\gamma[BH + n(H^2 - h^2)]}{b}$$

For a given embankment geometry (including design height) and soil strength profile, the maximum bearing pressure q_u can be established from [3], [5*a*], and [5*b*] above together with Figs. 10 and 11. The average applied pressure can be established from [6], and hence the ratio q_u/q_a may be determined.

If nominal foundation strength and unit weight parameters are used, then q_u/q_a represents the maximum conventional factor of safety that could be achieved for a heavily reinforced embankment. If factored foundation strength and unit weight parameters are used, then a ratio of q_u/q_a greater than one implies that a reinforced embankment could be constructed to the desired height under undrained conditions. If the ratio q_u/q_a is less than one, then no amount of reinforcement would be sufficient to allow undrained construction to the desired height for the conditions and partial load factors being considered. The application of this approach is illustrated in a later section.

Limit equilibrium analysis

The stability of both an unreinforced and a steel-reinforced embankment can be evaluated using a simple limit equilibrium analysis as described below.

The basic assumptions are given as follows (see Fig. 12).
(*i*) The embankment is constructed under undrained conditions ($\phi = 0$).
(*ii*) The failure surface in the foundation can be approximated by a circular arc.
(*iii*) The embankment can be modelled by means of an equivalent surcharge pressure on the foundation and a horizontal thrust (due to earth pressure within the embankment). This approach is the same as that adopted by Jewell (1982, 1988).
(*iv*) The reinforcement is located within the fill material and not directly on top of the foundation. (This constraint ensures that frictional resistance can be developed both above and below the reinforcement.)
(*v*) The pullout resistance of the reinforcement is related to the frictional resistance developed on the steel strips and is determined by integrating the shear resistance of fill–reinforcement interface over the length of reinforcement under consideration.

$$[7] \quad T = MS_s \int_0^L \sigma_N \tan\phi_s \, dx$$

where
T is pullout resistance,
M is 2 if the strips are embedded in fill (it represents the forces developed on the top and bottom of the strip),
S_S (=w/S) is an area reduction factor to allow for the fact that the steel strips do not cover the entire planar area,
w is width of each steel strip,
S is centre to centre spacing between steel strips,
σ_N is normal stress due to fill above reinforcement,
$\tan\phi_s$ is tangent of apparent fill–reinforcement interface friction angle ϕ_s,
dx is increment of reinforcement length, and
L is length of reinforcement (contained within failure circle).

If smooth steel strips are used, then ϕ_s is the steel–soil friction angle. The pullout resistance of smooth steel strips can be quite low, especially for small thicknesses of fill. To increase pullout resistance, ribbed steel strips are commonly used in Reinforced Earth™ (*R*) walls. For these strips the pullout resistance comes from a combination of passive resistance of the soil adjacent to the ribs (which act like small "anchors") and direct friction between the smooth section of the reinforcement and the fill. The passive resistance of soil developed in front of anchors in granular material is dependent on the dilatancy of the soil (e.g., see Rowe and Davis 1982) which, in turn, is related to stress level. Thus the friction angle ϕ_s deduced from pullout tests of ribbed strips does not represent a true friction angle but rather an "apparent friction angle", which incorporates the two components of resistance. Based on empirical experience related to Reinforced Earth™ (*R*) walls, the apparent friction angle for these ribbed strips can be given by

$$[8a] \quad \tan\phi_s \simeq F_0 \left(1 - \frac{N}{N_0}\right) + \tan\phi \left(\frac{N}{N_0}\right) \cdots \quad N \le N_0$$

$$[8b] \quad \tan\phi_s \simeq \tan\phi \qquad N > N_0$$

where
$F_0 = 1.2 + \log_{10}\mathrm{CU}$, where $\mathrm{CU} = D_{60}/D_{10}$ = coefficient of uniformity of the embankment fill (in the absence of accurate measurements a minimum value of $F_0 = 1.5$ was adopted in accordance with Reinforced Earth™ (*R*) recommendations),
N is normal stress due to fill above reinforcing strip,
N_0 is normal stress due to height of 6 m of fill, and
$\tan\phi$ is tangent of steel–fill interface friction angle.
For limit state design, [8*a*] and [8*b*] are multiplied by partial factors (see example calculations).

The limit equilibrium method considers moment equilibrium about the circle centre under consideration. The overturning moments are made up of two components, one being that due to the embankment fill weight contained within the slip circle (W_1x_1, W_2x_2 as shown in Fig. 12), and the other due to a horizontal thrust force from the earth pressure in the fill (Pz_p in Fig. 12). The restoring moments are derived from the reinforcement and shear strength of the clay foundation along the failure surface.

A closed-form expression is used to compute the resisting moment due to the clay foundation along some trial slip surface which has an origin (x_c,z_c) relative to the toe of the embankment (see Fig. 12). This expression allows one to consider either a homogeneous deposit or a deposit where the shear strength varies with depth. For the purposes of the following discussion, it is convenient to define a quantity called the equilibrium ratio, which is simply the ratio of the restoring moments to the overturning moments viz:

$$[9] \quad \text{equilibrium ratio (ERAT)} = \frac{\text{restoring moments}}{\text{overturning moments}} = \frac{\text{MRR} + \text{MRSOIL}}{\text{MOFILL} + \text{MOPT}}$$

where for limit equilibrium we require ERAT = 1.
MRR is the restoring moment due to limiting force in the steel, i.e., MRR = z_R T, where z_R is the vertical distance from the centre of the trial circle to the reinforcement (see Fig. 12), and T is the minimum of

(i) the sum of thrust force in fill plus clay–fill interface shear = $P + T_s$

$$= \frac{K_A \gamma H^2}{2} + \alpha c_{uo}\left[x_c + R\sin\left(\frac{\theta}{2}\right)\right]$$

where α is clay–fill interface adhesion factor and K_A is coefficient of active earth pressure

(ii) the pullout capacity of the reinforcement

$$= 2S_s \int_0^{x_c + R\sin(\theta/2)} \sigma_N \tan\phi_s \, dx \quad \text{(based on [7])}$$

(iii) allowable reinforcement force (governed by yield strength of the steel), F_A is the allowable force per unit (metre) width.

$$= F_A = F_y/S$$

F_y is the yield strength of the reinforcement strip; and S is the spacing between strips.

MRSOIL is the restoring moment due to the mobilized shear strength along the circular failure surface in the clay foundation

$$\text{MRSOIL} = \int_{-\theta/2}^{\theta/2} c_u(z) R^2 d\delta$$

$$= c_{uo} R^2\theta - \rho_c Z_0 R^2\theta + 2R^3 \rho_c \sin\frac{\theta}{2}$$

where

$$c_u(z) = c_{uo} + (R\cos\delta - Z_0)\rho_c.$$

MOFILL is the sum of overturning moments due to embankment fill self-weight applied to the clay foundation. The embankment fill is subdivided into a number of regions to simplify computations.

$$\text{MOFILL} = W_1(x_1 - x_c) + W_2(x_2 - x_c) + \cdots$$

$$= \sum_{i=1}^{m} W_i (x_i - x_c)$$

$$= W_1 X_1 + W_2 X_2 + \cdots$$

$$= \sum_{i=1}^{m} W_i X_i$$

where

W_i is the weight due to embankment fill of region i,

x_i is the x coordinate of centroid of region i,

x_c is the circle centre,

$X_i = x_i - x_c$, i.e., the horizontal distance from the centre of the trial circle to centroid of region being considered, and

m is the number of regions.

MOPT is the overturning moment due to horizontal thrust pressure (force) in the embankment fill

$$\text{MOPT} = 0.5 K_A \gamma H^2 \left(Z_0 - \frac{H}{3}\right)$$

For an unreinforced embankment MRR = 0 and all other terms are as defined above.

As with conventional limit equilibrium analyses, a number of trial slip circles are examined with a view to finding the minimum value of equilibrium ratio.

If nominal strength parameters are used, then ERAT corresponds to the conventional factor of safety for an unreinforced embankment. If factored parameters are used in a limit-state design of a reinforced embankment, then a value of ERAT greater than unity means that too much reinforcement has been used and, for example, the spacing S between steel strips could be increased until ERAT is equal to one. Conversely, if ERAT is less than unity, it implies that there is insufficient reinforcement and the spacing between strips should be decreased until ERAT becomes one.

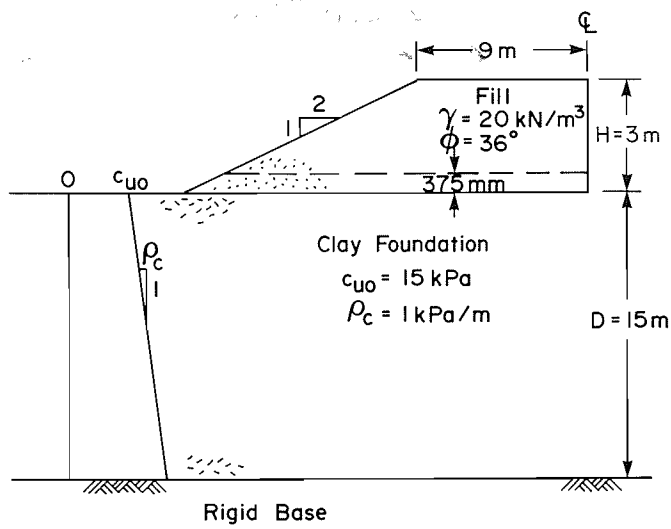

FIG. 13. Reinforced embankment example. The steel reinforcement consists of ribbed strips 50 mm × 5 mm with a spacing S = 375 mm, E = 200 000 MPa, σ_y = 350 MPa, and σ_{UTS} = 490 MPa.

Application

To illustrate the application of the proposed approach, consideration will be given to the design of a 3 m high, 18 m wide (crest width) embankment with 2:1 side slopes to be constructed on a 15 m deep soft clay deposit with a nominal shear strength profile that increases with depth, from c_{uo} = 15 kPa at the surface, at a rate of ρ_c = 1 kPa/m (see Fig. 13). The fill is to have a unit weight of 20 kN/m^3 and a friction angle of 36°.

In this example, the embankment fill and clay foundation parameters are factored according to the Ontario Highway Bridge Design Code (Ministry of Transportation of Ontario 1983). This need not be the scheme adopted and it is up to the discretion of the designer, as to how he or she wishes to incorporate partial factors or factor of safety when using the methods of analysis described in the previous sections. The symbols used are as previously defined.

The basic parameters are as follows:

(i) clay: c_{uo} = 15 kPa, ρ_c = 1 kPa/m

(ii) fill: γ = 20 kN/m^3, ϕ = 36°

(iii) geometry: D = 15 m, B = 2 × 9 m = 18 m
n = 2

The factored parameters from the Ontario Highway Bridge Design Code (Ministry of Transportation of Ontario 1983) are

c^*_{uo} = 15 × 0.65 = 9.75 kPa,

ρ^*_c = 1 × 0.65 = 0.65 kPa/m,

ϕ_f = $\tan^{-1}$(tan 36 × 0.8) = 30.2°, and

γ_f = 20 × 1.25 = 25 kN/m^3.

where * denotes that this is a factored foundation parameter and the subscript f denotes a factored fill parameter.

Step 1: stability of embankment without reinforcement

Based on the factored parameters, a limit equilibrium

analysis of the unreinforced embankment gives a value of equilibrium ratio ERAT of about 0.8. This implies that the unreinforced embankment cannot be constructed to the desired height of 3 m with an adequate factor of safety based on the Ontario Highway Bridge Design Code (Ministry of Transportation of Ontario 1983) and partial load factors (the maximum allowable height unreinforced would be 2.46 m).

Step 2: bearing capacity limit for heavily reinforced embankments

Taking the design height $H = 3$ m, and referring to Figs. 9 and 13, from [1]

$$h = \left(\frac{2+\pi)c^*_{uo}}{\gamma}\right)$$

$$= \left(\frac{2+\pi)9.75}{25}\right) = 2\ m$$

from [2]

$$b = B + 2n(H - h)$$
$$= 18 + 2(2)\ (3 - 2) = 22\ \text{m}$$
$$nh = 2 \times 2 = 4\ \text{m}$$
$$\frac{\rho^*_c b}{c^*_{uo}} = \frac{(0.65)\,(22)}{9.75} = 1.47$$

from Fig. 11

$$\frac{d}{b} \simeq 0.40$$

therefore $d = 0.4(22) = 8.8$ m.

From [4]

$$x = \min(d,D) = \min(8.8,15) = 8.8 \qquad > nh = 4$$

Therefore from [5*a*]

$$q_s = \frac{n\gamma h^2}{2x} = \frac{(2)(25)(2)^2}{2(8.8)} = 11.4\ \text{kPa}$$

$$\frac{b}{D} = \frac{22}{15} = 1.47$$

From Fig. 10

$$N_c \simeq 7$$

From [3]

$$q_u = N_c c^*_{uo} + q_s = 7(9.75) + 11.4 = 79.6\ \text{kPa}$$

From [6]

$$q_a = \frac{\gamma[BH + n(H^2 - h^2)]}{b}$$
$$= \frac{25\{18(3) + 2[(3)^2 - (2)^2]\}}{22}$$
$$= 72.7\ \text{kPa}$$
$$\frac{q_u}{q_a} = \frac{79.6}{72.7} = 1.1$$

Since q_u/q_a is greater than unity, this calculation indicates that the desired design height can be achieved (under undrained conditions) by adding sufficient reinforcement; the question that remains is how much reinforcement is required. This is addressed in step 3. It is noted in passing that the critical height H_c, which gives a ratio q_u/q_a equal to unity, is 3.3 m.

Since the calculations were performed using factored parameters, H_c corresponds to the maximum allowable height to which a heavily reinforced embankment could be constructed over this soil deposit based on limit state design concepts and the Ontario Highway Bridge Design Code (Ministry of Transportation of Ontario 1983) recommended partial load factors.

Step 3: stability of embankments with reinforcement

An initial estimate must be made concerning the properties and spacing of the ribbed steel strip reinforcement. In this case the steel strips are taken to be 50 mm wide and 5 mm thick, with a centre to centre spacing of 375 mm. The strips are to be located 375 mm above the clay–fill interface (this number is arbitrary and could be less; however, there should be enough clean granular fill above the clay to ensure that both the top and bottom of the steel strip are in contact with clean granular fill). In many cases it may be useful to install a separation geotextile between the fill and the foundation. Since this geotextile is for separation and not reinforcement, an appropriate lower strength geotextile could be used.

The reinforcement–fill frictional properties used in the relationship defining the apparent friction angle (eqs. [8*a*] and [8*b*]) are determined as follows. Given $F_0 = 1.5$, $N_0 = 6$ m $\times$ 20 kN/m^3 = 120 kN/m^2 i.e., 120 kPa, and $\phi = 36°$, the factored parameters F^*_0, N^*_0, and ϕ^* can be obtained by applying appropriate partial factors:

$$F^*_0 = F_\phi \times F_0$$

In this case the partial factor F_ϕ, applied to the interface strength terms F_0, is given by

$$F_\phi = 0.8 \times 0.8 \times 0.8 = 0.512$$

where one of the 0.8 represents factoring of strength, one represents factoring down of γ, since in this instance the self-weight improves stability; and one accounts for the fact that the unit weight has been factored up as a load, i.e., γ design = 1.25γ.

$$F^*_0 = 0.512 \times 1.5 \simeq 0.768$$
$$N^*_0 = 1.25 \times N_0$$
$$= 1.25 \times 120 = 150\ \text{kN/m}^2 = 150\ \text{kPa}$$
(factored up by load factor of 1.25)

$$\tan\phi^* = F_\phi \times \tan\phi$$

Therefore, $\phi^* = \tan^{-1}(F_\phi \tan\phi)$
$= \tan^{-1}(0.512 \times \tan 36°)$
$= 20.4°$.

In the analyses, the factored parameters F^*_0, N^*_0 and ϕ^* are substituted for F_0, N_0 and ϕ, respectively, in [8*a*] and [8*b*] to obtain $\tan\phi_s$ for use in [9].

The pullout resistance is then determined from [7], where S_s, the area reduction factor, is given by:

$$S_s = \frac{w}{S} = \frac{50}{375} = 0.1333$$

where S is centre to centre strip spacing, and w is width of steel strip.

The factored allowable reinforcement force is determined using the steel strip properties given in Fig. 13 and appropriate Ontario Highway Bridge Design Code (Ministry of Transportation of Ontario 1983) clauses governing the allowable strength of tension members. This gives $T_y = 63.2$ kN/strip. Therefore, the allowable force per metre width = number of steel strips $\times\ T_y$

$$= \frac{1000}{375} \times 63.2$$

$$\simeq 168 \text{ kN/m}$$

Again, the following factored properties are used in the analysis: (*i*) clay foundation and embankment fill properties; (*ii*) the factored reinforcement–fill friction properties; and (*iii*) the factored yield force in the reinforcement.

Taking $H = 3$ m, a search for the critical (lowest) equilibrium rate ERAT yields a value of 0.977. Since this is less than unity, the amount of reinforcement is not quite sufficient. One could reduce the spacing slightly and repeat the calculation until ERAT = 1 was obtained. However, given the conservative nature of the load factors and partial factors adopted, for the purpose of the present example, this spacing is judged to be sufficient.

A finite-element analysis was performed to assess the allowable height for this amount of reinforcement and factored parameters. The input parameters used in the finite-element analysis were factored in the same manner as previously described above. It was found that the allowable height was 3.1 m. The corresponding value based on limit equilibrium (for this reinforcement and ERAT = 1) is 2.9 m, indicating that the simple limit equilibrium calculation is slightly conservative compared with the finite-element analysis.

As noted in the introduction, the authors are not aware of any well-documented field cases involving steel strip reinforcement for embankments on soft soil. Both the limit equilibrium and finite-element analyses provide generally consistent results that suggest that there are cases where steel reinforcement could substantially improve embankment stability. It is hoped that the present paper will generate interest concerning the potential use of steel strip reinforcement and that future field experience can be used to refine the design methodology and analysis described herein.

Conclusion

Results of finite-element analyses have shown that reinforcement in the form of steel strips can substantially improve the undrained stability of embankments constructed on soft clayey deposits where there is an increase in strength with depth. It has been shown that the behaviour of these steel-reinforced embankments is highly dependent on the amount of reinforcement used and the properties of the underlying foundation soil.

A simple approach for the analysis and design of the embankment has been presented and has been illustrated by means of a worked example. The design established on the basis of simple consideration of bearing capacity and limit equilibrium was checked against a full finite-element analysis and found to be slightly conservative. Additional checking of the methodology against observed field performance is recommended.

Acknowledgements

Partial funding for the research reported herein was provided by Reinforced Earth (Australia) Pty Ltd. Additional funding was provided by the Natural Sciences and Engineering Research Council of Canada under grant A1009. The research was conducted in collaboration with the Civil and Mining Engineering Foundation of the University of Sydney. The authors are particularly indebted to Mr. M. Boyd of Reinforced Earth Australia; Professors H.G. Poulos and J.R. Booker and Dr. J.C. Small of the Department of Civil Engineering, The University of Sydney, for the review of the preliminary work and for many valuable discussions.

Carter, J.P. 1985. AFENA—A general finite element program, user's manual. School of Civil and Mining Engineering, University of Sydney, N.S.W. 2006, Australia.

Davis, E.H. 1968. Theories of plasticity and failure of soil masses. *In* Soil mechanics—selected topics. *Edited by* I.K. Lee. Butterworth Publishers, Stoneham, Mass. pp. 341–380.

Duncan, J.M., Schaefer, V.R., Franks, L.W., and Collins, S.A. 1987. Design and performance of a reinforced embankment for Mohicanville Dike No. 2 in Ohio. Transportation Research Record 1153, pp. 15–25.

Elias, V., and Johnson, E.G. 1982. The use of a reinforced earth slab to reduce embankment loads at Auke Bay, Alaska. State of Alaska, Department of Transportation and Public Facilities Report.

Fowler, J., Peters, J., and Franks, L. 1986. Influence of reinforcement modulus on design construction of Mohicanville Dike No. 2. *In* Proceedings, 3rd International Conference on Geotextiles, Vienna, Austria. Nov. 7–11. *Edited by* Organizing Committee. Österreichischer Ingenieur und Architektenverein, Vienna. pp. 267–272.

Fukuoka, M., and Goto, M. 1988. Design and construction of steel bars with anchor plates applying to strengthen the high embankment on soft ground. Proceedings of the International Geotechnical Symposium on Theory and Practice of Earth Reinforcement, Fukuoka, Japan, Oct. 5–7. *Edited by* T. Yamanouchi, N. Miura, and H. Ochiai. Balkema, Rotterdam. pp. 389-394.

Jewell, R.A. 1982. A limit equilibrium design method for reinforced embankments on soft soil. *In* Proceedings of the 2nd International Conference on Geotextiles, Las Vegas, Nev. Aug. 1–6. *Edited by* Organizing Committee. Industrial Fabrics Association International, St. Paul, Minn. Vol. 3, pp. 671–676.

Jewell, R.A. 1988. The mechanics of reinforced embankments on soft soils. Geotextiles & Geomembranes, **7**: 237–274.

Matar, M., and Salençon, J. 1977 Capacité portante à une semelle filante sur sol purement cohérent d'épaisseur limitée et de cohésion variable avec la profondeur. Annales de l'Institut Technique du Bâtiment et des Travaux Publics, Supplément No. 352 (Juillet–Août 1977), Série: Sols et Fondations, No. 143, pp. 95–107.

Ministry of Transportation of Ontario. 1983. Ontario Highway Bridge Design Code (and Commentary). Highway Engineering Division, Ministry of Transportation of Ontario, Toronto.

Mylleville, B.L.J., and Rowe, R.K. 1988. Steel reinforced embankments on soft clay foundations. *In* Proceedings of the International Geotechnical Symposium on Theory and Practise of Earth Reinforcement, Fukuoka, Japan, Oct. 5–7. *Edited by* T. Yamanouchi, N. Miura, and H. Ochiai. Balkema, Rotterdam. pp. 437–442.

Mylleville, B.L.J., and Rowe, R.K. 1993. Hubrey Road: A geosynthetic reinforced embankment constructed on a soft organic deposit. *In* Proceedings of Geosynthetic '93, March 30–April 1, Vancouver. *Edited by* R. Bathurst. Industrial Fabrics Association International, St. Paul, Minn. pp. 297–310.

Naylor, D.J., and Richards, H. 1978. Slipping strip analysis of reinforced earth. International Journal for Numerical and Analytical Methods in Geomechanics, **2**: 343–366.

Rowe, R.K., and Davis, E.H. 1982. The design of anchor plates in sand. Géotechnique, **32**: 9–23.

Rowe, R.K., and Mylleville, B.L.J. 1988. The analysis of steel reinforced embankments on soft clay foundations. *In*

Proceedings of the 6th International Conference on Numerical Methods in Geomechancis, Innsbruck, Austria. April 11–15. *Edited by* G. Swoboda. Balkema, Rotterdam. pp. 1273–1278.

Rowe, R.K., and Soderman, K.L. 1984. Comparison of predicted and observed behaviour of two test embankments. International Journal of Geotextiles and Geomembranes, **1**: 143–160.

Rowe, R.K., and Soderman, K.L. 1985. An approximate method for estimating the stability of geotextile-reinforced embankments. Canadian Geotechnical Journal, **22**: 392–398.

Rowe, R.K., and Soderman, K.L. 1987*a*. Reinforcement of embankments on soils whose strength increases with depth. *In* Proceedings of Geosynthetics '87 Conference, New Orleans, La. Feb. 24–25. *Edited by* Organizing Committee. Industrial Fabrics Association International, St. Paul, Minn. pp. 266–277.

Rowe, R.K., and Soderman, K.L. 1987*b*. Stabilization of very soft soils using high strength geosynthetics: The role of finite element analyses. International Journal of Geotextiles and Geomembranes, **6**: 53–80.

Rowe, R.K., MacLean, M.D., and Soderman, K.L. 1984. Analysis of a geotextile reinforced embankment constructed on peat. Canadian Geotechnical Journal, **21**: 563–576.

Vidal, H. 1969. The principle of reinforced earth. Highway Research Record, No. 282, pp. 1–16.

Ziekiewicz, O.C. 1977. The finite element method. 3rd ed. McGraw Hill, London.